Computations of Nonlinear Ship Waves

S.W. Song and R.E. Baddour

1. Introduction

Computations of ship waves found in the literature can be classified in two categories: linear and nonlinear approximations. The linear computations are based on either solving the Neumann-Kelvin or Dawson's linear ship wave problem. The nonlinear computations found in the literature are basically using Dawson's linear free surface condition iteratively on the computed wave surface to obtain a nonlinear solution to the exact ship wave problem. The numerical method used to solve the Neumann-Kelvin linear problem is the so-called Kelvin source method. Dawson's linear problem is solved by Rankine source method. Constant element techniques are generally used in both the Neumann-Kelvin and Rankine source methods. Literature review shows that solutions to the problem lack satisfactory agreement. Recently a new nonlinear theory based on domain transformation and nonlinear perturbation has been developed by Pawlowski for solving the ship wave problem.

In the present paper the exact free surface condition satisfied on the actual free surface is transformed, through a Taylor's series expansion, to the undisturbed fluid free surface. An iterative method based on the direct boundary integral theory and the linear element techniques is developed to solve the transformed nonlinear ship wave problem. In order to compare the present method with existing ones and to discuss the Neumann-Kelvin and Dawson's linear models, a new linear free surface condition, as a special case of the transformed nonlinear free surface condition, is also derived and implemented. The present numerical method is also used to solve the Neumann-Kelvin and Dawson's linear ship wave problems for comparison purposes.

2. Formulations and Numerical Method

The free surface condition in the nonlinear boundary value problem solved in the present study is obtained by transforming the free surface condition of the exact ship wave problem from being satisfied on the actual free surface to being satisfied on the undisturbed fluid free surface through a Taylor's series expansion. To first order in η it is given as:

$$(1+\eta\frac{\partial}{\partial z})[g\frac{\partial\phi}{\partial z}+\frac{1}{2}\nabla\phi\cdot\nabla(\nabla\phi\cdot\nabla\phi)]=0,\quad on\ z=0, \tag{1}$$

where ϕ is the velocity potential, and η represents the wave elevation.

The wave elevation η is also expressed by the velocity potential on the undisturbed free surface through Taylor's series expansion up to the first order in η, which is given as:

$$\eta = \frac{U^2 - (|\nabla\phi|)^2}{2(g + \nabla\phi\frac{\partial}{\partial z}\nabla\phi)}, \quad z = 0, \tag{2}$$

where U is the constant velocity of the ship.

The convergence of Taylor's series expansion of the free surface condition, equation (1), has been analysed by using Pawlowski's nonlinear perturbation theory. The free surface condition given by equation (1) is satisfied on $z = 0$. This brings many advantages to the numerical procedures, especially to the iterative scheme developed in this work.

The ship wave boundary value problem with the nonlinear free surface condition given by equation (1) is solved by an iterative method. The scheme solves a nonlinear boundary value problem by solving a series of linear boundary value problems. In each iteration condition (1) is linearized by the sum of the velocity potentials obtained from the previous iterations plus an increment. The solution of the linearized boundary value problem is obtained by a numerical solver which is developed by using the direct boundary integral theory and linear element techniques. In the first step an initial value is needed to start the iteration. Theoretically, the initial value can be chosen arbitrarily.

In order to compare the present method with existing ones and discuss the limitations in using the Neumann-Kelvin and Dawson's linear free surface conditions, a new linearized surface condition based on condition (1) is obtained. It is in the form:

$$A\frac{\partial^2\phi}{\partial\ell^2} + B\frac{\partial\phi}{\partial\ell} + C\frac{\partial\phi}{\partial z} + D\frac{\partial^2\phi}{\partial\ell\partial z} + E\frac{\partial^3\phi}{\partial\ell^2\partial z} = H, \quad on\ z = 0. \tag{3}$$

The coefficients A, B, C, D, E, and H in this equation are functions of the double-body potential and the double-body streamline ℓ on $z = 0$.

The direct boundary integral formulation distributes the velocity potentials and their normal derivatives on the boundary of the considered domain. The fundamental equation in the direct boundary integral formulation is in the form:

$$\int_S \phi(q)\frac{\partial}{\partial n(q)}[\frac{1}{r(p,q)}]dS(q) = \int_S \frac{1}{r(p,q)}\frac{\partial\phi(q)}{\partial n(q)}dS(q), \tag{4}$$

where $\phi(q)$ represents the velocity potential at point q, $n(q)$ represents the unit normal to boundary S at point q, and $r(p,q)$ is the distance between the collocation point q and the field point p.

The linear element techniques distribute the unknowns on the nodes of the surface mesh and linearly vary the unknowns over each element. The complexity of the linear element algorithm is much higher than that of the constant element algorithm found in the literature. However, the disadvantages inherent in the use of constant element algorithm, such as the collocation points being away from the actual boundary, the variables between panels being discontinuous, and the panelization being

inaccurate, are removed. Therefore, more accurate computational results can be obtained by applying the linear element techniques.

3. Results and Conclusions

Computations using the present linear and nonlinear models have been carried out for the Wigley and Series 60, $C_b = 0.6$, ship hulls. Fig.1 shows the comparison of wave resistance coefficient C_w between the present linear computations and the linear computations found in the literature based on solving either the Neumann-Kelvin linear model or Dawson's linear model. The experimental data are also plotted in the same figure. Fig.1 shows that the present linear method matches the linear computations based on solving the Neumann-Kelvin and Dawson's linear ship wave problems, and all of them match the experimental data for the Wigley hull.

In Fig.2, C_w for Series 60 hull obtained by using the present numerical method for solving the Neumann-Kelvin, Dawson's and the present linear ship wave problems are presented. Unlike the Wigley hull case, differences are found between the present linear model and the Neumann-Kelvin and Dawson's linear models. The present linear computation matches the experimental data fairly well.

Fig.3 shows the nonlinear computations. The present nonlinear computation matches the results obtained based on Pawlowski's nonlinear perturbation theory and both sets match the experimental measurements very well.

In Fig.4, a comparison between the present nonlinear computations and experimental measurements of wave profile along Series 60 hull waterline is presented.

As a result of the study the following conclusions are drawn:

1. Both the Neumann-Kelvin and Dawson's linear model can only be applied to thin ships. Even though the wave resistance results obtained by using Dawson's linear free surface condition are improved in comparison with the results obtained by using the Neumann-Kelvin linear free surface condition, Dawson's linear free surface condition still can not model realistic ships.

2. The present linear model is obtained by keeping the zero and first orders in η in the Taylor's series expansion, it gives good predictions for both the Wigley and Series 60 hulls.

3. The present nonlinear computations match the results obtained based on Pawlowski nonlinear theory and they all match the experimental measurements very well.

4. Numerical experiments show that the numerical algorithms used in this work are robust, efficient, and accurate in solving the ship wave problem.

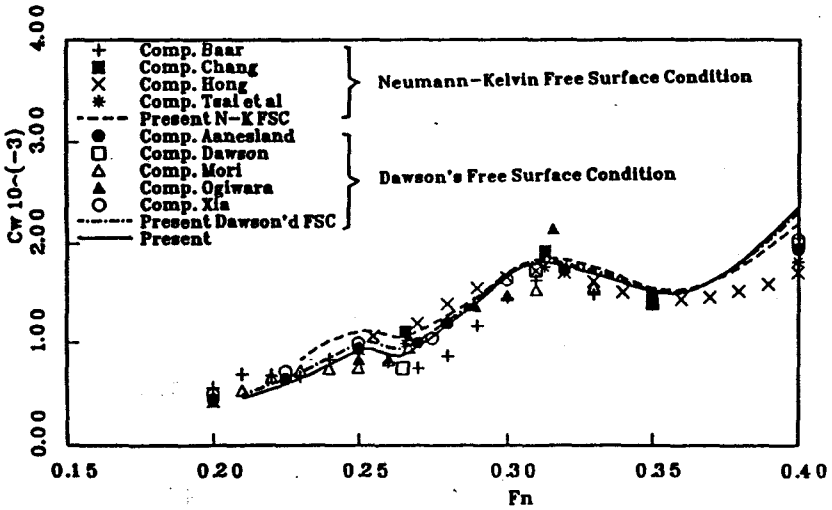

Fig. 1 Comparison of wave resistance coefficient C_w for Wigley hull

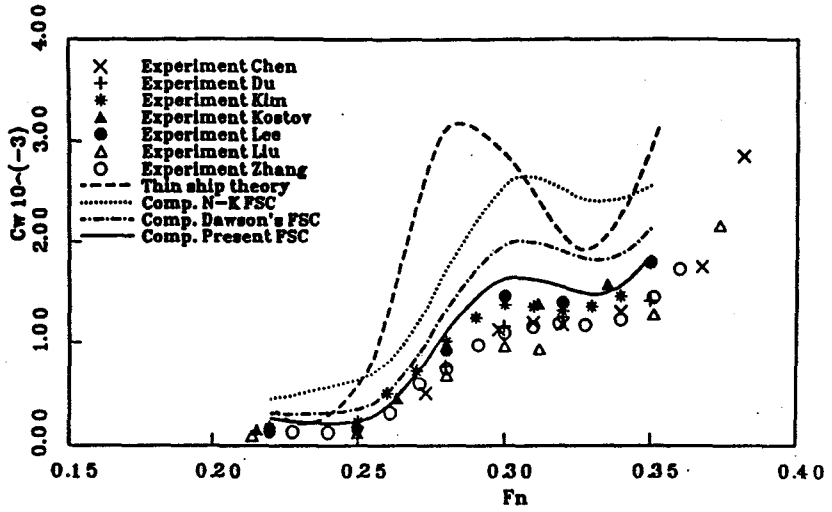

Fig. 2 Comparison of wave resistance coefficient C_w for Series 60 hull

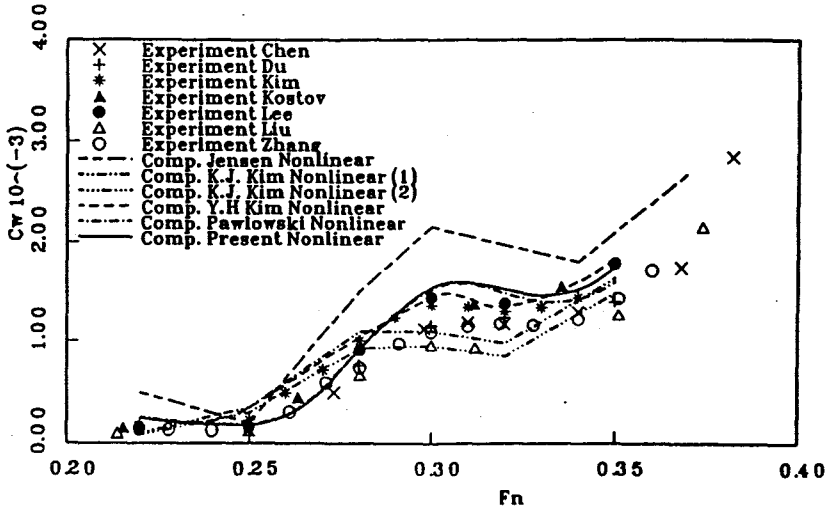

Fig. 3 Comparison of nonlinear C_w for Series 60 hull

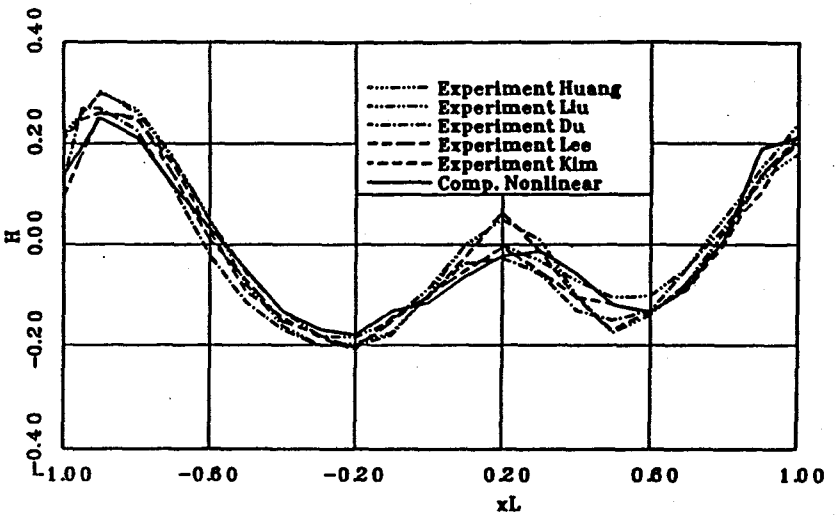

Fig. 4 Comparison of nonlinear wave profiles for Series 60 hull (Fn=0.28)